

Synthesis and properties of differently charged chemiluminescent acridinium ester labels†

Cite this: *Org. Biomol. Chem.*, 2013, **11**, 1026

Anand Natrajan* and David Sharpe

Chemiluminescent acridinium dimethylphenyl esters containing *N*-sulfofpropyl groups in the acridinium ring are highly sensitive, hydrophilic labels that are used in automated immunoassays for clinical diagnostics. Light emission from these labels is triggered with alkaline peroxide in the presence of a cationic surfactant. At physiological pH, *N*-sulfofpropyl acridinium esters exist as water adducts that are commonly referred to as pseudobases. Pseudobase formation, which results from addition of water to the zwitterionic *N*-sulfofpropyl acridinium ring, neutralizes the positive charge on the acridinium nitrogen and imparts a net negative charge to the label due to the sulfonate moiety. As a consequence, *N*-sulfofpropyl acridinium ester conjugates of small molecule haptens as well as large molecules such as proteins gain negative charges at neutral pH. In the current study, we describe the synthesis and properties of two new hydrophilic acridinium dimethylphenyl ester labels where the net charge in the labels was altered. In one label, the structure of the hydrophilic *N*-alkyl group attached to the acridinium ring was changed so that the pseudobase of the label contains no net charge. In the second acridinium ester, two additional negative charges in the form of sulfofpropyl groups were added to the acridinium ring to make this label's pseudobase strongly anionic. Chemiluminescence measurements of these labels, as well as their conjugates of an antibody with a neutral pI, indicate that acridinium ester charge while having a modest effect on emission kinetics has little influence on light output. However, our results demonstrate that acridinium ester charge can affect protein pI, apparent chemiluminescence stability and non-specific binding of protein conjugates to microparticles. These results emphasize the need for careful consideration of acridinium ester charge in order to optimize reagent stability and performance in immunoassays. In the current study, we observed that for a neutral protein, an acridinium ester with a hydrophilic but charge-neutral *N*-alkyl group afforded faster light emission, lower non-specific binding and better chemiluminescence stability than an analogous label with an anionic *N*-alkyl group.

Received 9th November 2012,
Accepted 10th December 2012

DOI: 10.1039/c2ob27190g

www.rsc.org/obc

Introduction

Chemiluminescent acridinium dimethylphenyl esters containing *N*-sulfofpropyl groups in the acridinium ring are highly sensitive, hydrophilic labels that are used in automated immunoassays for clinical diagnostics.¹ Conjugates of these acridinium esters are commonly used in conjunction with magnetic microparticles in immunoassays for analytical measurements of a wide range of clinically important analytes.^{1a,c,d} Light emission from these labels and their conjugates is triggered with alkaline peroxide in the presence of the cationic surfactant cetyltrimethylammonium chloride (CTAC). While exact details of the light emission pathway are still not

completely understood, excited state acridone is believed to be the light emitting species that is presumably formed from addition of peroxide to C-9 of the acridinium ring (see Fig. 1, panel A for the numbering system) followed by scission of the phenolic ester bond.² Dioxetane and/or dioxetanone intermediates have been proposed as immediate precursors of excited state acridone.²

The surfactant CTAC influences light emission from acridinium dimethylphenyl esters by two separate mechanisms.³ In the presence of CTAC, emission times from acridinium esters and their conjugates are compressed from approximately 60 seconds to ≤ 5 seconds for most labels and their conjugates. CTAC also enhances light yield by 3–4 fold by facilitating formation of the dioxetane and/or dioxetanone intermediates. These surfactant-mediated effects on light emission enable fast assays with improved sensitivity and they require the binding of the acridinium ring to CTAC micelles through a combination of hydrophobic and charge interactions.⁴ However, a label's hydrophobicity and charge can exacerbate

Siemens Healthcare Diagnostics, Advanced Technology and Pre-Development, 333 Coney Street, East Walpole, MA 02032, USA. E-mail: anand.natrajan@siemens.com; Fax: +1-508-660-4591; Tel: +1-508-660-4582

†Electronic supplementary information (ESI) available. See DOI: 10.1039/c2ob27190g

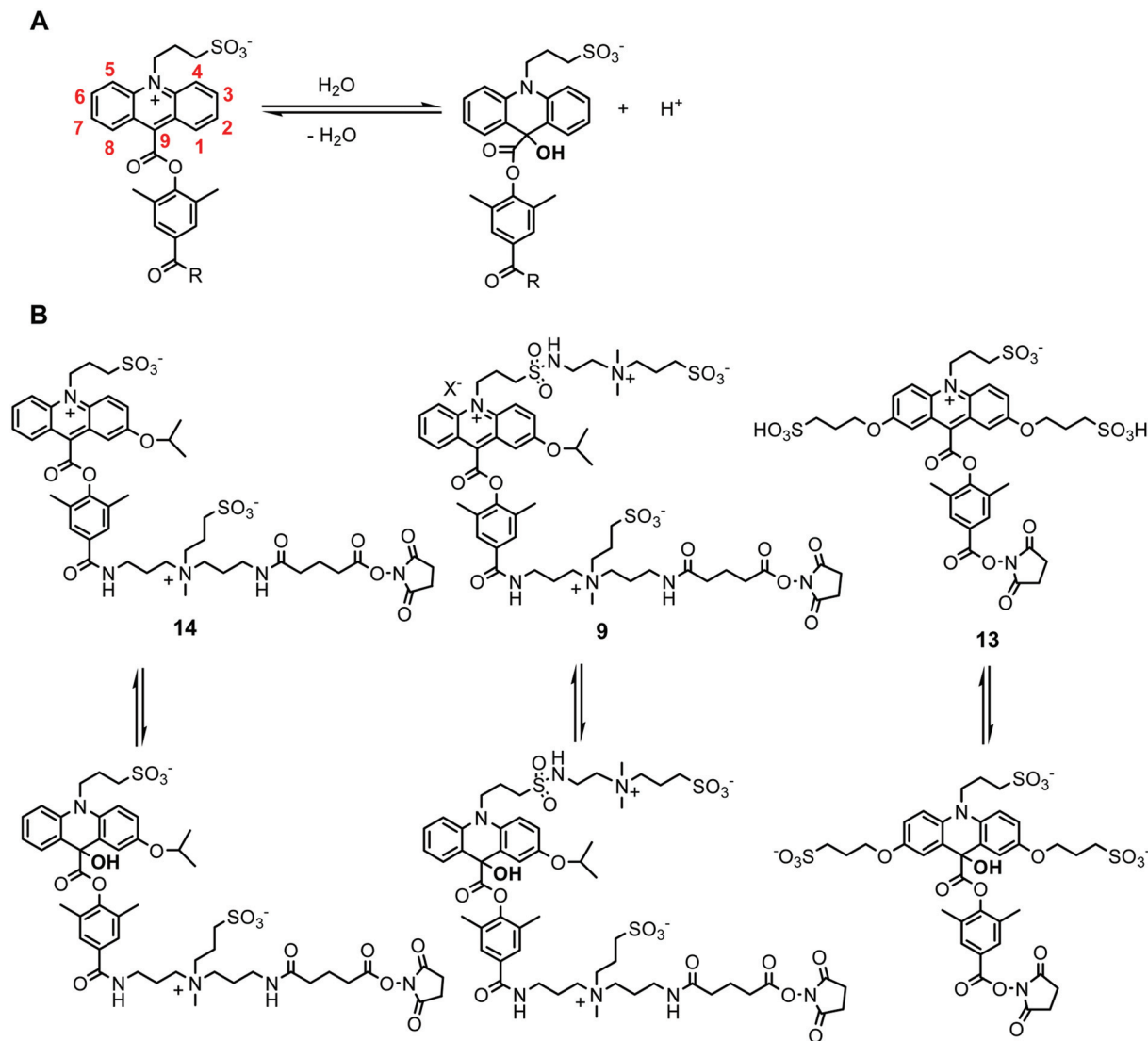


Fig. 1 Panel A: Acridinium–pseudobase equilibrium of an *N*-sulfopropyl acridinium dimethylphenyl ester. Addition of water to C-9 neutralizes the positive charge on the acridinium nitrogen and imparts a net negative charge to the label. Panel B: Structures of acridinium esters and their pseudobases of an anionic acridinium ester **14** and charge-neutral and strongly anionic acridinium esters **9** and **13** respectively synthesized in the current study.

its non-specific binding to microparticles and can compromise assay sensitivity in immunoassays. We recently reported⁴ that the adverse effects of a hydrophobic acridinium ring can be mitigated by incorporating a highly polar, sulfobetaine zwitterion linker in the phenolic ester. An example of such an optimized structure is shown in Fig. 1 (compound **14**, panel B). This acridinium ester contains a relatively hydrophobic acridinium ring with an electron-donating isopropoxy group at C-2 and a phenolic ester with a sulfobetaine zwitterion linker. The isopropoxy group in **14** increases light output approximately twofold compared to the corresponding unsubstituted acridinium ester. Segregating the hydrophobic and hydrophilic structural features in the acridinium ring and phenol respectively in **14** ensures low non-specific binding of the label to microparticles without disrupting the critical influence of CTAC on its light emission.

At physiological pH, acridinium esters with various *N*-alkyl groups exist as water adducts that are commonly referred to as pseudobases.^{4,5} Pseudobase formation, which results from the addition of water to the central ring of the acridinium ester, neutralizes the positive charge on the acridinium nitrogen. Consequently, triggering light emission from acridinium esters requires an acid pre-treatment step which restores the electrophilic center at C-9 by converting the pseudobase to the acridinium form (Fig. 1, panel A). The pK_a of acridinium to pseudobase transition of acridinium esters depends upon the electronics of the acridinium ring and can be measured by spectrophotometry.^{4,5b} For most acridinium esters, the pK_a of pseudobase formation is <7 .^{4,6} Pseudobase formation in *N*-sulfopropyl acridinium esters (such as **14**) imparts a net negative charge to the label due to the sulfonate moiety in the pseudobase (Fig. 1, panel A). As a consequence, *N*-sulfopropyl

acridinium ester conjugates of small molecule haptens as well as large molecules such as proteins gain negative charges at $\text{pH} \geq 7$.

Despite the widespread use of *N*-sulfopropyl acridinium esters and analogous compounds⁷ in immunoassays, no study has addressed the question of whether these negatively charged labels are really optimal in every situation? To answer this question, in the present study, we have investigated how overall charge of the acridinium ring impacts the properties of chemiluminescent acridinium dimethylphenyl ester labels. We describe the syntheses and properties of two new acridinium esters with differently charged (charge-neutral or strongly anionic) acridinium rings in their respective pseudobases (Fig. 1, panel B, compounds **9** and **13**). We also illustrate how these labels influence the properties of a monoclonal antibody with a neutral pI in comparison to a conventional acridinium ester label with an *N*-sulfopropyl acridinium ring (Fig. 1, panel B, compound **14**). Our results indicate that overall charge of chemiluminescent acridinium ester labels can influence properties such as pI, non-specific binding and apparent chemiluminescence stability of protein conjugates. All are important factors that can affect reagent performance in immunoassays.

Results and discussion

Synthesis of acridinium ester labels and conjugates (Fig. 2 and 3, S1–S9,† Table 1)

At first glance, the synthesis of an acridinium ester whose pseudobase is charge-neutral appears trivial given that *N*-methyl acridinium phenyl esters and their derivatives were described more than 20 years ago.^{2a,b,8} The pseudobases of these compounds do not contain any charge. However, the acridinium ring in these compounds is very hydrophobic and overall aqueous solubility of these labels is quite low making them generally unsuitable for labeling hydrophobic haptens.^{1a} When first described,^{1a} acridinium dimethylphenyl esters with *N*-sulfopropyl groups in the acridinium ring represented an advance over *N*-methyl acridinium esters because they alleviated the solubility problems of the latter and yet were sufficiently hydrophobic for efficient binding to CTAC micelles. Also importantly, the *N*-sulfopropyl acridinium esters could be conveniently synthesized by *N*-alkylation of their acridine ester precursors with the potent alkylating reagent 1,3-propane sultone.^{1a} The main drawback of the original synthetic protocol was that the *N*-alkylation reaction had to be conducted at elevated temperatures with the toxic alkylating reagent serving the dual role of reactant and solvent. This was necessitated by the very poor reactivity of the acridine nitrogen of acridine dimethylphenyl esters towards alkylating reagents. Recently,⁹ we reported that the *N*-alkylation of acridine dimethylphenyl esters with and without various alkoxy groups in the acridine ring with 1,3-propane sultone proceeds very efficiently in highly polar, aprotic, room temperature ionic liquids with significantly reduced quantities of the alkylating reagent. Given the generally very poor reactivity of the acridine nitrogen

towards alkylating reagents¹⁰ with the exception of 1,3-propane sultone or strong methylating reagents, we decided to use the easily-introduced *N*-sulfopropyl group (using our new synthetic protocol⁹) as the scaffold to construct an acridinium ester with a charge-neutral but highly polar *N*-alkyl group (compound **9**, Fig. 1).

The synthetic scheme for compound **9** is illustrated in Fig. 2. Compound **1**, which is a synthetic intermediate of compound **14**⁴ with an *N*-sulfopropyl acridinium ring, was used as a starting point for the synthesis. Initially, we attempted to directly convert compound **1** to compound **5** by activating the sulfonate moiety in **1** followed by condensation with the zwitterionic amine derivative **4** whose synthesis we described recently.^{1d} Caddick and coworkers¹¹ have described a convenient method to convert sulfonate salts of heterocyclic amines to sulfonamides and pentafluorophenyl sulfonate esters using triphenylphosphine and trifluoromethanesulfonic anhydride for sulfonate activation. Treatment of compound **1** with these reagents followed by pentafluorophenol however failed to give the pentafluorophenyl ester **3a**. The poor solubility of the zwitterionic amine **4** in the solvent (dichloromethane) used for activation¹¹ of the sulfonate **1** also precluded any chance of reaction between **1** and **4**. We next resorted to the conventional method for activating sulfonates which was to convert **1** to the sulfonyl chloride using neat thionyl chloride. This activation reaction required careful control of reaction time to prevent cleavage of the entire sulfonate moiety and its replacement with chlorine. Short reaction times (≤ 30 minutes) minimized this side reaction although attempted condensation of the sulfonyl chloride with the zwitterionic amine **4** in dimethyl sulfoxide led mainly to hydrolysis of the moisture sensitive sulfonyl chloride and no evidence of product **5**.

With these failed attempts to directly convert **1** to compound **5**, we decided to use a two step approach as illustrated in Fig. 2. Condensation of the sulfonyl chloride of **1** with *N,N*-dimethylethylenediamine in acetonitrile led to the sulfonamide **2** which was isolated in 70% yield by preparative HPLC. The tertiary amine in **2** was then alkylated with 1,3-propane sultone in the ionic liquid 1-butyl-3-methylimidazolium hexafluorophosphate [BMIM][PF₆] to give compound **5**. This alkylation reaction in the ionic liquid gave complete conversion to product **5** with no trace of starting material by HPLC analysis. As an alternative to this two step approach, we also examined conversion of the sulfonate of **1** to the more stable fluorophenyl esters **3a** and **3b** and their subsequent coupling to the zwitterionic amine **4**. This approach appeared attractive for several reasons. First, sulfonyl pentafluorophenyl esters are much more stable than sulfonyl chlorides and published studies suggest that they can be coupled to amines even under aqueous conditions.¹² Second, recent publications have demonstrated that the reactivity of fluorophenyl esters of carboxylic acids towards amine nucleophiles can be tuned by the number of fluorines in the fluorophenyl ester.¹³ If the reactivity of sulfonyl fluorophenyl esters can be tuned in a similar manner, it can provide synthetic access to various

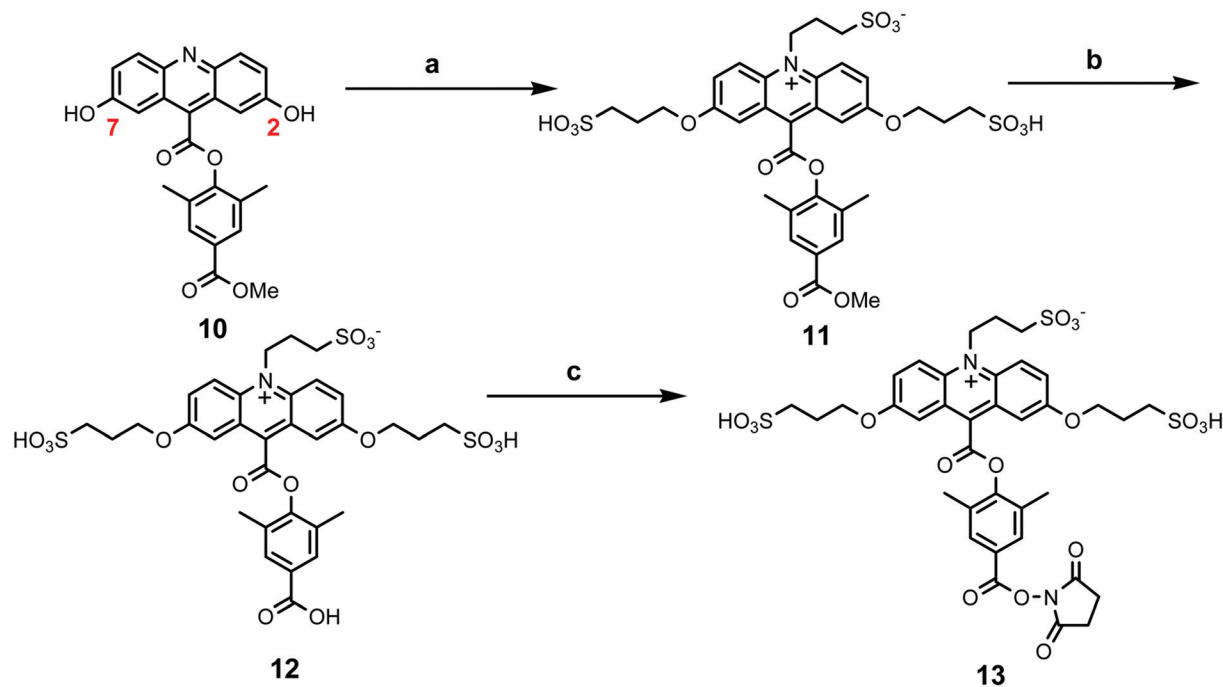


Fig. 3 Synthetic scheme for compound 13. Reagents: (a) 1,3-propane sultone, sodium carbonate, [BMIM][PF₆]; (b) 1 M HCl; (c) TSTU, diisopropylethylamine, DMF.

Table 1 Anti-HBsAg antibody labeling with acridinium esters 9, 13 and 14

Acridinium ester label	Input, equivalents of acridinium ester in labeling reaction	No. of labels by mass spectroscopy	Specific activity (RLUs per mole $\times 10^{-19}$)
9	5	3.0	6.0
9	10	5.0	6.4
13	5	3.0	6.3
13	10	6.0	6.1
14	5	3.0	6.2
14	10	6.0	4.2

after preparative HPLC and proved to be quite stable showing little signs of decomposition at room temperature. We next investigated reaction conditions for the coupling of these fluorophenyl esters to the amine 4. While attempted coupling of the pentafluorophenyl ester 3a to 4 under aqueous conditions (0.25 M sodium bicarbonate–dimethyl sulfoxide) led mainly to hydrolysis of the pentafluorophenyl ester, coupling in neat dimethyl sulfoxide at 65–100 °C led to 60% conversion to product 5 with an isolated yield of 40% after preparative HPLC. The 2',6'-difluorophenyl ester 3b proved to be much less reactive and showed no evidence of hydrolysis or coupling to 4 under aqueous conditions at room temperature. However in dimethyl sulfoxide at ~100 °C, 70% conversion to product 5 was observed with an isolated yield of 50% by HPLC. Our results suggest that for aliphatic sulfonates, 2,6-difluorophenyl esters may be superior to pentafluorophenyl esters due to their increased stability especially in aqueous solvents. The synthetic routes that we have outlined should provide access to various *N*-propylsulfonamide-substituted acridinium compounds that would normally be very difficult to synthesize using alternate chemistry.

Completion of the rest of the synthesis of acridinium ester 9 was relatively straightforward using chemistry we have described previously.^{3,4} The methyl ester in 5 was cleaved by acid hydrolysis and the carboxylic acid derivative 6 was isolated in 72% yield by preparative HPLC. Condensation of 6 with the zwitterionic diamine linker 7³ was achieved using standard *N*-hydroxysuccinimide ester chemistry for activation of the carboxylate 6. Compound 8, which was isolated in 85% yield by preparative HPLC, was then condensed with glutaric anhydride and the glutarate intermediate was subsequently converted to the target *N*-hydroxysuccinimide ester 9.

Synthesis of the strongly anionic label 13 was achieved as illustrated in Fig. 3. To preserve the strongly anionic nature of this compound, we decided not to introduce the neutral zwitterionic linker 7 present in compounds 13 and 14 which have more hydrophobic acridinium rings compared to 13. Previously described 2,7-dihydroxyacridine ester derivative 10¹⁴ was alkylated in one step at both the two phenolic groups as well as the acridine nitrogen with 1,3-propane sultone in the ionic liquid [BMIM][PF₆] with sodium carbonate or potassium carbonate as the base. Conversion of 10 to the trisulfonated product 11 required the use of acid-free 1,3-propane sultone and strict anhydrous conditions. The use of commercial 1,3-propane sultone directly without distillation led to the formation of mixtures of sulfonates that were difficult to separate. Synthesis of the target 13 was completed by acid hydrolysis of the methyl ester in 11 which was isolated in 55% yield by preparative HPLC (two steps), followed by conversion of the carboxylate 12 to the *N*-hydroxysuccinimide ester 13 using standard chemistry. The final product 13 was isolated in 93% yield by preparative HPLC. HPLC analyses of all the

intermediates and final compounds of Fig. 2 and 3 are shown in the ESI (Fig. S1–S9†).

Protein conjugates of the labels **9**, **13** and **14** were prepared as described in the Experimental section using an in-house, murine, anti-HBsAg monoclonal antibody with a neutral pI (HBsAg = hepatitis B surface antigen). All three labels displayed similar reactivity towards the protein and the extent of label incorporation was very similar as described in the Experimental section (Table 1). Using an input of 5–10 equivalents of the acridinium ester labels led to incorporation of 3–6 labels for each label as measured by MALDI-TOF (matrix-assisted laser desorption ionization-time of flight) mass spectroscopy.

Emission spectra, pH titrations and chemiluminescence measurements (Fig. 4–7, S10†)

Emission spectra of acridinium ester labels **9**, **13** and **14** are shown in Fig. 4 along with the structures of the putative acridones that are formed during the chemiluminescent reactions of these labels. The emission spectra were recorded using a spectral camera in a mostly aqueous medium (>90% water) as described in the Experimental section. The emission spectrum of **14** was reported in our previous study⁴ and is included here for reference. The emission spectrum of the charge-neutral label **9** was observed to be identical to that of **14** with an emission maximum centered at 458 nm. Both these acridinium esters contain the same C-2 isopropoxy functional group in the acridinium ring which is mainly responsible for the bathochromic shift in their emission spectra when compared to unsubstituted *N*-sulfopropyl acridinium esters whose emission maxima are typically observed at 430 nm.^{1c,4} The bulky, zwitterion-substituted, *N*-propylsulfonamide group in **9** was not expected to affect its emission spectrum and Fig. 4 confirms this expectation. On the other hand, the emission spectrum of

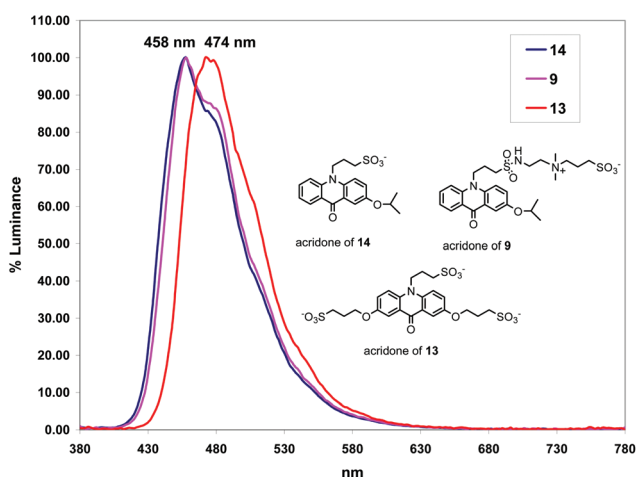


Fig. 4 Emission spectra of acridinium esters **9**, **13** and **14**. Structures of the putative acridones are shown for the three acridinium esters. Due to similar C-2 alkoxy substitution, the emission spectrum of compound **9** was observed to be identical to that of compound **14**. Compound **13** showed a bathochromic shift in its emission spectrum due to two electron-donating ether oxygens at C-2 and C-7.

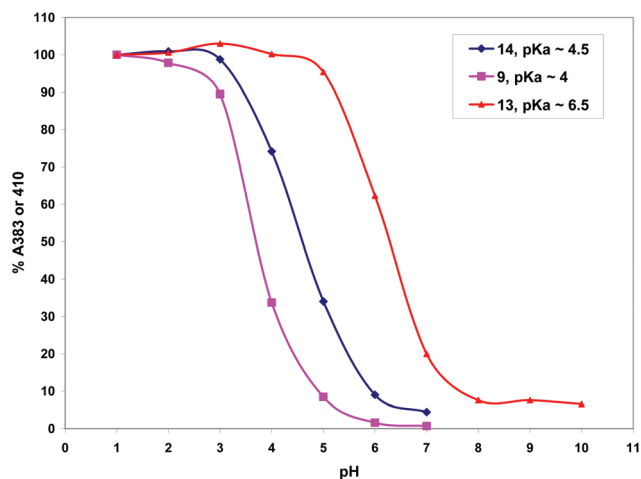


Fig. 5 pH titrations illustrating conversion of the acridinium form to the pseudobase for compounds **9**, **13** and **14**. The bulky *N*-alkyl group in compound **9** shifted the pK_a to acidic pH compared to compound **14**. The strongly anionic label **13** showed a shift in pK_a to basic pH owing to increased electron donation by the two ether oxygens at C-2 and C-7.

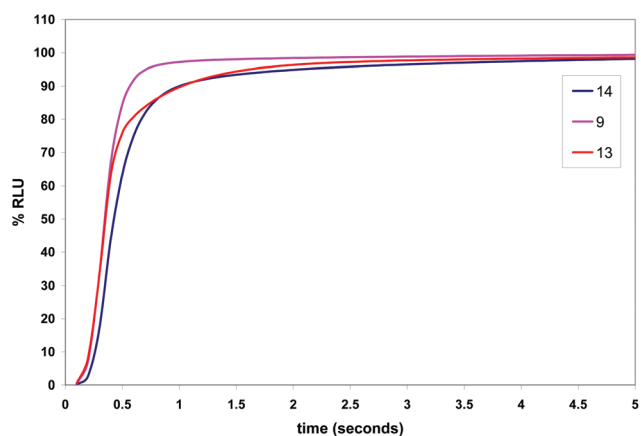


Fig. 6 Chemiluminescence emission profiles of compounds **9**, **13** and **14** in the presence of cetyltrimethylammonium chloride (CTAC). All three acridinium esters showed rapid light emission in the presence of the cationic surfactant with similar light yield (RLU = relative light unit).

compound **13** showed a bathochromic shift in the emission spectrum with a maximum centered at 474 nm. This result is consistent with our earlier observations on the chemiluminescence emission spectra of electron-rich, 2,7-dialkoxy-substituted acridinium esters that also showed bathochromic shifts compared to monoalkoxy-substituted compounds.^{1c}

Acridinium esters, at acidic pH, show strong long-wavelength absorption bands due to the acridinium chromophore that disappears as the pH is raised due to formation of the pseudobase.^{4,5} Formation of the pseudobase by addition of water at C-9 (Fig. 1, panel A) results in disruption in conjugation of the acridinium ring with concomitant loss of the long wavelength absorption band. Pseudobase formation can be followed by spectrophotometry and the pK_a of the acridinium to pseudobase transition can be determined by varying the pH.⁴ The pK_a of the acridinium to pseudobase transition

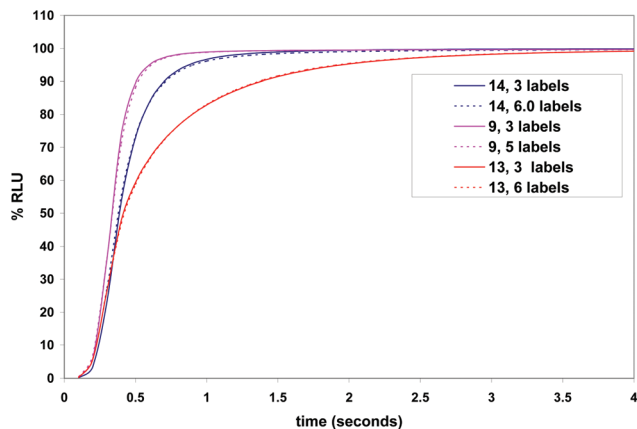


Fig. 7 Chemiluminescence emission profiles of anti-HBsAg antibody conjugates of acridinium esters **9**, **13** and **14** in the presence of CTAC. Label density was observed not to affect emission kinetics or light yield for each label. Emission kinetics of the conjugates increased in the order **9** > **14** > **13** (HBsAg = hepatitis B surface antigen).

of acridinium esters typically reflects the electron density at C-9 of the acridinium ring. Electron donating groups at C-2 and/or C-7 decrease the electron density at C-9 and shift the pK_a for pseudobase formation to basic pH.^{4,6} pH titrations of the acridinium esters **9**, **13** and **14** are shown in Fig. 5. As expected, the 2,7-dialkoxy-substituted acridinium ester **13** displayed a shift in the pK_a for pseudobase formation to 6.5 compared to **14** ($pK_a \sim 4.5$) which has a single C-2 alkoxy group. Surprisingly, acridinium ester **9**, despite being substituted with the same C-2 isopropoxy group as **14**, exhibited a shift in the pK_a to acidic pH ($pK_a \sim 4$). These observations suggest that the bulky *N*-alkyl group in **9** disfavors a flat acridinium ring due to steric congestion. Formation of the pseudobase presumably relieves this steric congestion. We have observed that other acridinium esters with bulky *N*-alkyl groups also exhibit shifts in their pK_a for pseudobase formation to acidic pH (unpublished data). Our observations also imply that the pK_a of pseudobase formation of acridinium esters is indicative of the electron density at C-9 only when the *N*-alkyl groups in the acridinium ring are identical.

Chemiluminescence measurements of the labels **9**, **13** and **14** as well as their anti-HBsAg antibody conjugates were carried out as described previously.^{3,4} In a typical experiment, 1–2 mg mL⁻¹ solutions of HPLC-purified labels and the corresponding protein conjugates of these compounds were serially diluted in phosphate buffer to approximately 0.5 nM (nM = nanomolar, 10⁻⁹ M) for the free labels, and approximately 0.2 nM for the protein conjugates as described in the Experimental section. Chemiluminescence from 0.01 mL of each diluted sample was triggered by the addition of 0.3 mL each of 0.1 M nitric acid containing 0.5% hydrogen peroxide followed by the addition of 0.25 M sodium hydroxide. In experiments with CTAC, the surfactant was included in the second reagent (0.25 M sodium hydroxide) at five times its reported critical micelle concentration (CMC) in water.^{3,4} Light was collected for a total of two minutes, integrated at 0.5 second intervals in the

absence of CTAC and for 10 seconds integrated at 0.1 s intervals in the presence of CTAC. The light collection time was sufficiently long for complete emission under all conditions.

The emission profiles of the labels **9**, **13** and **14** in the presence of CTAC and in its absence are shown in Fig. 6 and S10 (ESI[†]) respectively. Consistent with our earlier observations with other acridinium ester labels,^{3,4} light emission in the absence of CTAC was slow requiring more than a minute for complete emission as illustrated in Fig. S10.[†] In the presence of CTAC, these emission times were compressed to ≤ 5 seconds (Fig. 6). These results indicate that the acridinium rings of the three labels partition strongly into CTAC micelles.⁴ Despite differences in their pK_a for pseudobase formation, in the presence of excess peroxide ions, emission kinetics of the three labels were quite similar. Specific activity of the labels in the presence of CTAC was also observed to be quite similar with observed specific activities of 5.9, 5.4 and 4.6 $\times 10^{19}$ RLU per mole (RLU = relative light unit) for **9**, **13** and **14** respectively (average of three replicates). Total light yield was increased approximately 3-fold for each label in the presence of CTAC.^{3,4}

Chemiluminescence emission profiles of the protein conjugates are shown in Fig. 7. Light emission was again observed to be rapid for all three labels and was not affected by label density. Modest differences in the emission kinetics were noted for the three labels with the conjugates of **9** showing the fastest light emission (>90% emission in 0.5 second) whereas conjugates of the strongly anionic label **13** were the slowest emitters (>90% emission in 2 seconds). Emission kinetics of the conjugates of label **14** fell in between requiring one second for >90% emission. Despite these differences in emission kinetics, the specific activities of the labels in the conjugates were observed to be quite similar as illustrated in Table 1 (Experimental section).

In an earlier empirical study, we reported that acridinium esters with methoxy groups at C-2 and/or C-7 display the greatest increase in light yield (2–3-fold) compared to other regioisomeric, methoxy-substituted acridinium esters.^{1c} It has been suggested in recent publications that competition between hydroperoxide ions and hydroxide ions for reaction at C-9 of acridinium esters drives the light and dark reactions respectively^{2d} and that these dark reactions are suppressed for 2,7-dimethoxy-substituted acridinium esters.¹⁵ The pK_a of acridinium to pseudobase transition is shifted progressively to more basic pH for these alkoxy-substituted esters as observed in this study and our earlier reports.⁴ Intuitively, an increase in pK_a should reduce the electrophilic character at C-9 and increase discrimination between more nucleophilic hydroperoxide ions (light reaction) rather than hydroxide ions (dark reaction). However, as observed for compound **9**, a decrease in pK_a is not always correlated with a drop in light yield. Similarly, an increase in pK_a for compound **13** did not increase light output. Decomposition of dioxetane intermediates formed in the chemiluminescent reaction of acridinium esters is postulated to occur *via* electron transfer from the acridine nitrogen^{2b,16} in a mechanism that is analogous to Schuster's CIEEL (chemically-initiated electron exchange luminescence) mechanism.¹⁷

This electron transfer mechanism may be more efficient for electron rich C-2 and/or C-7 alkoxy-substituted acridinium esters and may explain why compounds **9**, **13** and **14** have the same light output despite the observed differences in their pK_a for pseudobase formation.

Conjugate pI, chemiluminescence stability and non-specific binding (Fig. 8, 9, S11,† Table 2)

The acridinium rings of the labels **9**, **13** and **14** have different charge characteristics in their respective pseudobases and we examined their impact on protein pI, chemiluminescence stability as well as non-specific binding to magnetic microparticles that are commonly used in immunoassays.

To study the effect of these differently charged labels on protein pI, we selected a monoclonal antibody with a neutral pI (an in-house anti-HBsAg antibody) so that small perturbations in the charge of the protein caused by acridinium ester labeling could be more easily measured. Isoelectric focusing (IEF) gel electrophoresis is a commonly-used technique¹⁸ to measure protein pI and we used this method to study the impact of the three labels **9**, **13** and **14** on the pI of the anti-HBsAg antibody conjugates (Fig. 8). As shown in Fig. 8, labeling with the anionic label **14** and the strongly anionic label **13** shifted the pI of the protein from approximately 7 (lane 3) to approximately 5.5 for both labels (lanes 4–7). An increase in label density of either of these two labels showed more compact bands in the gel and a slightly greater shift in protein pI to acidic pH. Interestingly, although label **13** contains two additional negative charges compared to **14**, the IEF gel was

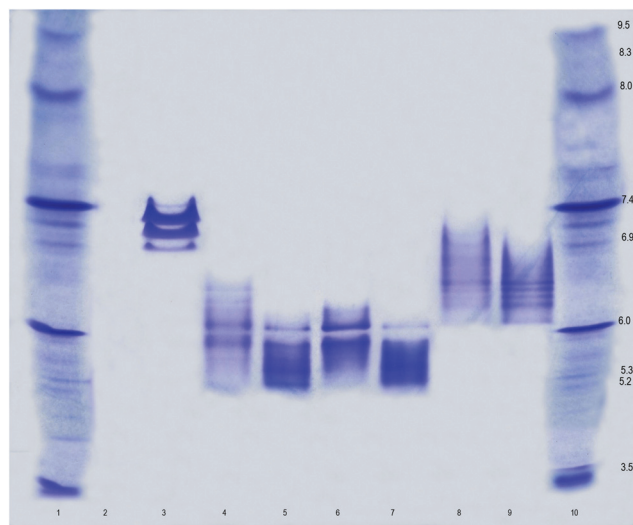


Fig. 8 Isoelectric focusing (IEF) gel of anti-HBsAg antibody conjugates with varying label density of acridinium esters **9**, **13** and **14**. The pI of the neutral antibody was shifted to acidic pH by the anionic labels **13** and **14** whereas the charge-neutral label **9** had a much smaller effect on protein pI. Lanes: (1) Novex IEF markers pH 3–10; (2) blank; (3) unlabeled antibody; (4) antibody conjugate of **13**, 3 labels; (5) antibody conjugate of **13**, 6 labels; (6) antibody conjugate of **14**, 3 labels; (7) antibody conjugate of **14**, 6.0 labels; (8) antibody conjugate of **9**, 3 labels; (9) antibody conjugate of **9**, 5 labels; (10) Novex IEF markers pH 3–10.

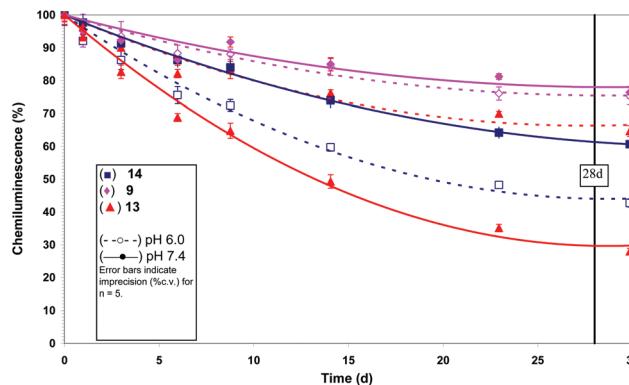


Fig. 9 Apparent chemiluminescence stability of anti-HBsAg antibody conjugates of labels **9**, **13** and **14** at pH 6.0 and pH 7.4 at 37 °C. Order of stability at pH 7.4 was observed to be **9** > **14** > **13** which was inversely correlated with the pK_a for pseudobase formation. Loss of chemiluminescence was not observed at either pH for all three labels at 4 °C (Fig. S11†).

unable to resolve any differences in pI in the conjugates of these two labels. Nevertheless, these results nicely illustrate the effect of these negatively charged labels on altering the pI of a neutral protein. In contrast, conjugates of the charge-neutral label **9** showed only a small shift in the pI of the protein to acidic pH (Fig. 8, lanes 8 and 9). The small shift is attributable to neutralization of some of the lysine residues on the protein caused by acridinium ester labeling. Thus, as predicted by its structural features, acridinium ester **9** contains no net charge in the acridinium ring and therefore had a minimal effect on protein pI.

Non-specific binding is a better reflection of molecular forces and we measured the non-specific binding of the more heavily-labeled conjugates (Tables 1 and 2) of **9**, **13** and **14** to three different types of magnetic particles that are commonly used in immunoassays. The particles selected were paramagnetic particles (PMPs) and two commercially available magnetic latex particles (MLPs). The PMPs used were 1–10 micron-sized iron(III) oxide particles, coated with a murine anti-fluorescein antibody which was coupled to the amino-silanzed particle surface using glutaraldehyde. The two MLPs (Dyna-beads® M-270 and M-280 particles) are available from a commercial vendor (Life Technologies). Both particles were 2.8 micron in size and were coated with streptavidin. The intrinsic, surface characteristics of the three types of particles are quite different because of different functional groups. PMPs contain amines on their surfaces whereas M-270 particles have hydrophilic carboxylate surfaces. The M-280 particles have a more hydrophobic surface with a tosylate-activated polystyrene coating (Experimental section). The two types of particles (PMPs and MLPs) were mixed with solutions of the acridinium ester conjugates and were then magnetically separated. They were subsequently washed twice, either with water or a surfactant solution, and then the chemiluminescence associated with the particles was measured. The ratio of this chemiluminescence value in comparison to the total chemiluminescence input is referred to fractional non-specific

Table 2 Fractional non-specific binding (FNSB) of acridinium ester (**9**, **13** and **14**) conjugates of anti-HBsAg antibody conjugates to three different magnetic microparticles measured on a Siemens Healthcare Diagnostics' ADVIA Centaur® system

Particles	14 , surfactant wash	14 , water wash	9 , surfactant wash	9 , water wash	13 , surfactant wash	13 , water wash
PMP	2.6×10^{-4}	2.4×10^{-4}	2.0×10^{-4}	2.1×10^{-4}	1.5×10^{-4}	1.4×10^{-4}
M-280-SA	1.3×10^{-4}	1.3×10^{-4}	6.6×10^{-5}	6.5×10^{-5}	4.9×10^{-5}	4.8×10^{-5}
M-270-SA	1.8×10^{-5}	1.8×10^{-5}	1.6×10^{-5}	1.6×10^{-5}	1.3×10^{-5}	0.9×10^{-5}

An input of 250–300 million RLUs, 5–6 labels per antibody corresponding to 1 picomole (1 picomole = 10^{-12} mole) of anti-HBsAg antibody conjugate and 70 μg of magnetic particles was used for each measurement (ten replicates). Surfactant wash corresponded to 0.8 mM Triton X-100 in PBS buffer, pH = 7.2. Abbreviations used: RLU = relative light unit; PMP = paramagnetic particle; M-280 and M-270 are commercial names of Dynabeads® (Life Technologies) with hydrophobic, tosyl-activated and hydrophilic carboxylate surfaces respectively; SA = streptavidin.

binding (FNSB) and reflects the resistance of the conjugate towards non-specific adsorption to the microparticles. The results of these measurements are tabulated in Table 2 and details are described in the Experimental section.

The results in Table 2 indicate that the FNSB values of the anti-HBsAg antibody conjugates of the labels **9**, **13** and **14** are not only dependent upon the charge of the acridinium ester label, but are also dependent upon the surface characteristics of the particles used in the measurements. For all three particles, regardless of the wash method (water or surfactant solution wash), FNSB of the labels decreased in the order **13** (strongly anionic) < **9** (charge-neutral) < **14** (anionic) defying conventional wisdom that non-ionic but hydrophilic functional groups are best for preventing protein adsorption to surfaces.¹⁹ The order of non-specific binding on the three types of particles was observed to be M-270 < M-280 < PMP for all three labels. Our results (Table 2) clearly demonstrate that acridinium ester charge does play an important role in dictating an important property of immunoassay reagents, *i.e.* non-specific binding. The strongly anionic label **13** appears to be the best label for a neutral protein based on these measurements but the addition of multiple negative charges may not be conducive to assay kinetics that use acidic proteins and particles with negatively charged surfaces such as the M-270 particles. Acridinium ester **9** may be the more attractive label for all three types of particles because it is charge-neutral yet hydrophilic with lower FNSB compared to the conventional anionic label **14**. This is most evident for the hydrophobic M-280 particles where the FNSB of **9** was twofold lower than **14**. This observation indicates that the acridine ring in the pseudobase of the charge-neutral label **9** is more hydrophilic than that of the anionic label **14**. Moreover, because of its unique structural features, as illustrated here with the neutral anti-HBsAg antibody, acridinium ester **9** is also not expected to alter the charge characteristics of proteins or small haptens.

Finally, we address acridinium ester chemiluminescence stability which is another important property of these labels for immunoassay applications. Acridinium ester instability is mostly attributed to hydrolysis of the phenolic ester linkage.⁸ Apparent chemiluminescence stability of anti-HBsAg antibody conjugates of the three labels **9**, **13** and **14** at pH = 6 and 7.4 at 37 °C is shown in Fig. 9. (No differences in stability could be discerned at 4 °C as shown in Fig. S11†) At pH 7.4, the order of stability was observed to be **9** > **14** > **13** which is also the order

of increasing pK_a for pseudobase formation for these labels. At first, these observations appear counterintuitive because an increase in pK_a should decrease the positive charge at C-9 and stabilize the adjacent phenolic ester linkage. However, at a given pH, an increase in pK_a for pseudobase formation causes a greater proportion of the acridinium ester to be in the acridinium form which is expected to be more susceptible to hydrolysis of the phenolic ester due to electron withdrawal from C-9. At pH 6, the charge-neutral label **9** with the lowest pK_a was still the most stable. But the order of stability of **13** and **14** was reversed with **13** (higher pK_a) being more stable than **14**. The apparent anomalous behavior of the strongly anionic label **13** may be the result of a combination of several factors. The label is expected to be strongly anionic (because of the two additional sulfonates in the acridinium ring at C-2 and C-7) at both pH = 6 and 7.4 so should repel negatively charged ions such as hydroxide ions more effectively than **14**. Yet, the acridinium ester also contains an electrophilic center at C-9 (in the acridinium form) that can destabilize the adjacent phenolic ester. At pH 6, a greater proportion of this acridinium ester is in the labile acridinium form compared to **14** (Fig. 5) but the concentration of hydroxide ions is low. At pH 7.4, the label is still strongly anionic but there is less labile acridinium form despite a greater concentration of hydroxide ions. These opposing factors may be responsible for the unusual pH-dependent stability behavior of **13** with the lower concentration of hydroxide ions and charge repulsion dictating better stability at pH = 6.0 despite a higher proportion of the labile acridinium form at this pH.

Conclusions

We have described the syntheses of two new, differently charged chemiluminescent acridinium dimethylphenyl esters **9** and **14** using synthetic routes that we developed specifically for assembling these unusual structures. Chemiluminescence measurements of these labels as well as their conjugates of a protein with a neutral pI indicated modest differences in emission kinetics but similar light yield. These differently charged labels however showed significant differences in both non-specific binding to microparticles and how they impacted protein pI. The labels also exhibited significant pH-dependent differences in chemiluminescence stability. Although not a focus of the current study, these differently charged acridinium ester labels may also influence other immunoassay

parameters such as binding rates and affinity constants of conjugates which will need to be evaluated separately for each assay. Our results emphasize the need for careful consideration of acridinium ester charge in order to optimize reagent stability and performance in immunoassays that use these chemiluminescent labels. Because a multitude of factors can affect immunoassay performance, empirical approaches such as the one we have described have considerable merit. During the course of this study, we have identified a new structural motif for acridinium esters, *i.e.* a charge-neutral, zwitterion-substituted hydrophilic acridinium ring, such as that in acridinium ester **13**. This new acridinium ester **13**, when conjugated to an antibody with a neutral pI showed faster emission kinetics, lower non-specific binding and better chemiluminescence stability when compared to the analogous label **14** with an *N*-sulfofpropyl acridinium ring.

Experimental

General

Chemicals were purchased from Sigma-Aldrich (Milwaukee, Wisconsin, USA) unless indicated otherwise. The ionic liquid [BMIM][PF₆] was dried under high vacuum over P₂O₅ prior to use.

All final acridinium esters and intermediates were analyzed and/or purified by HPLC using a Beckman-Coulter HPLC system. Flash chromatography was performed using an 'Auto-flash' system from ISCO. MALDI-TOF (matrix-assisted laser desorption ionization-time of flight) mass spectroscopy was performed using a Voyager DETM BiospectrometryTM Workstation from Perkin-Elmer. This is a benchtop instrument operating in the linear mode with a 1.2 meter ion path length, flight tube. Spectra were acquired in the positive ion mode. For small molecules, α -cyano-4-hydroxycinnamic acid was used as the matrix and spectra were acquired with an accelerating voltage of 20 000 volts and a delay time of 100 ns. For protein conjugates, sinapinic acid was used as the matrix and spectra were acquired with an accelerating voltage of 25 000 volts and a delay time of 85 ns.

For HRMS (high resolution mass spectra), samples were dissolved in HPLC-grade methanol and analyzed by direct-flow injection (injection volume = 5 μ L) electrospray ionization (ESI) on a Waters Qtof API US instrument in the positive ion mode. Optimized conditions were as follows: capillary = 3000 kV, cone = 35, source temperature = 120 °C, desolvation temperature = 350 °C. NMR spectra were recorded on a Varian 500 MHz spectrometer. IR spectra of neat samples were recorded on a Bruker TENSOR37 FT-IR spectrometer, ATR mode on a ZnSe crystal. UV-Visible spectra were recorded on a Beckman DU 7500 spectrophotometer. Chemiluminescence measurements were carried out using a Berthold Technologies' AutoLumat Plus LB953 luminometer.

1. Synthesis of acridinium esters (Fig. 2, 3 and Fig. S1–S9 ESI[†])

Compound 2. Compound **1** (108 mg, 0.19 mmole) in thionyl chloride (4 mL) was heated at 85 °C in an oil bath under a

nitrogen atmosphere for 30 minutes. The reaction was then cooled to room temperature, diluted with anhydrous toluene (5 mL) and concentrated under reduced pressure. The crude sulfonyl chloride was then treated with an ice-cold solution of *N,N*-dimethylethylenediamine (0.45 mL, 4.1 mmoles) in anhydrous MeCN (5 mL). The resulting solution was stirred at 0 °C under a nitrogen atmosphere. After 15 minutes, the reaction was analyzed by HPLC using a Phenomenex, C₁₈, 10 micron, 3.9 \times 300 mm column and a 30 minute gradient of 10 \rightarrow 100% MeCN–water (each with 0.05% TFA, TFA = trifluoroacetic acid) at a flow rate of 1.0 mL per minute and UV detection at 260 nm. Product was observed eluting at 17 minutes with no starting material at 19 minutes. The reaction was diluted with toluene (5 mL) and concentrated under reduced pressure. The crude reaction mixture was dissolved in DMF (4 mL) and purified by preparative HPLC using a YMC, 10 micron, C₁₈, 30 \times 250 mm column and a 30 minute gradient of 10 \rightarrow 100% MeCN–water (each with 0.05% TFA) at a solvent flow rate of 20 mL per minute and UV detection at 260 nm. The HPLC fractions containing product **2** were combined and concentrated under reduced pressure to yield a dark brown, sticky solid. Yield = 85 mg (70%). $\nu_{\max}/\text{cm}^{-1}$ 3424 (NH), 1752 and 1680 (CO), 1471, 1326, 1202, 1144. δ_{H} (500 MHz, CF₃COOD) 1.51 (d, 6H, *J* = 6.0), 2.54 (s, 6H), 2.88 (br s, 2H), 3.14 (s, 6H), 3.51 (br s, 2H), 3.80 (m, 4H), 4.07 (s, 3H), 4.91 (spt, 1H, *J* = 6.0), 5.73 (m, 2H), 7.87 (br s, 1H), 8.00 (s, 2H), 8.09 (m, 1H), 8.20 (m, 1H), 8.43 (m, 1H), 8.66 (m, 2H), 8.72 (d, 1H, *J* = 9.0). MALDI-TOF MS *m/z* 636.9 M⁺; HRMS *m/z* 636.2752 M⁺ (636.2743 calculated).

Compound 3a. Compound **1** (60 mg, 0.11 mmole) in thionyl chloride (2 mL) was heated at 85 °C in an oil bath under a nitrogen atmosphere for 30 minutes. The reaction was then cooled to room temperature and hexanes (30 mL) were added to precipitate the acid chloride. The hexanes were decanted and the residue was rinsed with additional hexanes (2 \times 10 mL). The crude sulfonyl chloride was then treated with an ice-cold solution of pentafluorophenol (94 mg, 0.51 mmole) and triethylamine (0.072 mL, 0.52 mmole) in anhydrous dichloromethane (5 mL). The resulting solution was stirred at 0 °C under a nitrogen atmosphere. After 1 hour, the reaction was analyzed by HPLC using a Phenomenex, C₁₈, 10 micron, 3.9 \times 300 mm column and a 30 minute gradient of 10 \rightarrow 100% MeCN–water (each with 0.05% TFA) at a flow rate of 1.0 mL per minute and UV detection at 260 nm. Compound **3a** was observed eluting at 25 minutes. The reaction was then concentrated under reduced pressure and the crude product was dissolved in MeCN (5 mL). The product was isolated by preparative HPLC as described for compound **2**. Yield = 55 mg (71%); red hygroscopic solid. $\nu_{\max}/\text{cm}^{-1}$ 1719 and 1688 (CO), 1522, 1474, 1367, 1325, 1186, 1147. δ_{H} (500 MHz, CF₃COOD) 1.47 (d, 6H, *J* = 6.0), 2.50 (s, 6H), 2.99 (br s, 2H), 4.02 (s, 3H), 4.07 (br s, 2H), 4.87 (spt, 1H, *J* = 6.0), 5.76 (br s, 2H), 7.83 (s, 1H), 7.95 (s, 2H), 8.06 (m, 1H), 8.17 (br d, 1H), 8.41 (m, 1H), 8.68 (m, 3H); δ_{F} (470 MHz, CF₃COOD) –154.3 (d, 2F, *J* = 16.9), –156.2 (t, 2F, *J* = 19.4), –163.0 (br t, 2F); MALDI-TOF MS *m/z* 732.7 M⁺; HRMS *m/z* 732.1707 M⁺ (732.1691 calculated).

Compound **3b** was prepared similarly. Yield = 58 mg (81%); red hygroscopic solid. $\nu_{\max}/\text{cm}^{-1}$ 1710 and 1687 (CO), 1480, 1377, 1198, 1164, 1145. δ_{H} (500 MHz, CF_3COOD) 1.47 (d, 6H, $J = 6.0$), 2.50 (s, 6H), 3.00 (br s, 2H), 4.03 (s, 3H), 4.05 (br s, 2H), 4.87 (spt, 1H, $J = 6.0$), 5.76 (br s, 2H), 7.04 (br t, 2H), 7.31 (m, 1H), 7.83 (s, 1H), 7.95 (s, 2H), 8.06 (br t, 1H), 8.17 (br d, 1H), 8.40 (m, 1H), 8.60 (br d, 3H). δ_{F} (470 MHz, CF_3COOD) -127.5 (br t, 2F). MALDI-TOF MS m/z 678.6; M^+ ; HRMS m/z 678.1970 M^+ (678.1973 calculated).

Compound 5

(a) *Synthesis from compound 3a.* A mixture of compound **3a** (40 mg, 0.055 mmole), compound **4** (29 mg, 0.138 mmole) and diisopropylethylamine (0.024 mL, 0.138 mmole) in dimethyl sulfoxide (2 mL) was heated at 65 °C under a nitrogen atmosphere for 2 hours. The reaction was then cooled to room temperature and analyzed by HPLC using a Phenomenex, C_{18} , 10 micron, 3.9×300 mm column and a 30 minute gradient of 10 → 100% MeCN–water (each with 0.05% TFA) at a flow rate of 1.0 mL per minute and UV detection at 260 nm. Product **5** was observed eluting at 17 minutes (60% conversion) with hydrolyzed starting material **1** (~40%) eluting at 19 minutes. The product **5** was purified by preparative HPLC as described for compound **2**. Yield = 17 mg (41%); red powder. $\nu_{\max}/\text{cm}^{-1}$ 3443 (NH), 1720 and 1688 (CO), 1470, 1326, 1200, 1147. δ_{H} (500 MHz, CF_3COOD) 1.48 (d, 6H, $J = 6.0$), 2.52 (br s, 8H), 2.85 (m, 2H), 3.27 (s, 6H), 3.39 (br t, 2H), 3.67–3.96 (m, 8H), 4.05 (s, 3H), 4.88 (spt, 1H, $J = 6.0$), 5.70 (br s, 2H), 7.84 (s, 1H), 7.97 (s, 2H), 8.06 (m, 1H), 8.18 (br d, 1H), 8.41 (m, 1H), 8.64 (m, 2H), 8.69 (d, 1H, $J = 8.5$). MALDI-TOF MS m/z 758.2 M^+ ; HRMS m/z 758.2753 M^+ (758.2781 calculated).

(b) *Synthesis from compound 3b.* A mixture of compound **3b** (30 mg, 0.044 mmole), compound **4** (46 mg, 0.22 mmole) and diisopropylethylamine (0.078 mL, 0.44 mmole) in dimethyl sulfoxide (3 mL) was heated at 95–100 °C under a nitrogen atmosphere for 16 hours. The reaction was then cooled to room temperature and analyzed by HPLC using a Phenomenex, C_{18} , 10 micron, 3.9×300 mm column and a 30 minute gradient of 10 → 100% MeCN–water (each with 0.05% TFA) at a flow rate of 1.0 mL per minute and UV detection at 260 nm. Product **5** was observed eluting at 17 minutes (70% conversion) with hydrolyzed starting material eluting **1** at 19 minutes (16%) and unreacted **3b** eluting at 24 minutes (13%). The product **5** was purified by preparative HPLC as described for compound **2**. Yield = 15 mg (50%); red hygroscopic solid.

(c) *Synthesis from compound 2.* A mixture of compound **2** (85 mg, 0.134 mmole), distilled 1,3-propane sultone (0.25 g, 2.05 mmoles) and 2,6-di-*tert*-butylpyridine (0.22 mL, 1.0 mmole) in [BMIM][PF₆] (1.0 mL) was heated at 150–155 °C in a sealed tube for 16 hours. The reaction was then cooled to room temperature and analyzed by HPLC using a Phenomenex, C_{18} , 10 micron, 3.9×300 mm column and a 30 minute gradient of 10 → 70% MeCN–water (each with 0.05% TFA) at a flow rate of 1.0 mL per minute and UV detection at 260 nm. Product **5** was observed eluting at 23 minutes with no trace of starting material **2** at 22 minutes. The reaction was transferred

to a 100 mL round bottom flask with methanol and concentrated under reduced pressure. The residue was washed with toluene (3×20 mL) and then dried under vacuum. Crude product **5** was used directly for the next reaction.

Compound 6. The crude product **5** from above was suspended in 1 M HCl (10 mL) and was refluxed under a nitrogen atmosphere. After 2 hours, the reaction was cooled to room temperature and analyzed by HPLC using a Phenomenex, C_{18} , 10 micron, 3.9×300 mm column and a 30 minute gradient of 10 → 70% MeCN–water (each with 0.05% TFA) at a flow rate of 1.0 mL per minute and UV detection at 260 nm. Clean conversion to product **6** eluting at 19 minutes was observed. The product was purified by preparative HPLC as described for compound **2**. Yield = 72 mg (72%); red hygroscopic solid. $\nu_{\max}/\text{cm}^{-1}$ 3435 (OH and NH), 1749 and 1667 (CO), 1483, 1308, 1200, 1152. δ_{H} (500 MHz, CF_3COOD) 1.51 (d, 6H, $J = 6.0$), 2.56 (br s, 8H), 2.87 (br s, 2H), 3.29 (s, 6H), 3.42 (br t, 2H), 3.69–4.02 (m, 8H), 4.92 (spt, 1H, $J = 6.0$), 5.74 (m, 2H), 7.87 (br s, 1H), 8.07 (s, 2H), 8.09 (m, 1H), 8.22 (m, 1H), 8.44 (m, 1H), 8.67 (m, 2H), 8.72 (d, 1H, $J = 8.0$). MALDI-TOF MS m/z 745.5 ($\text{M} + \text{H}$)⁺, HRMS m/z 744.2644 M^+ (744.2625 calculated).

Compound 8. A solution of compound **6** (72 mg, 0.097 mmole) in DMF (2 mL) and water (0.1 mL) was treated with diisopropylethylamine (0.034 mL, 0.2 mmole) and *N,N,N',N'*-tetramethyl-*O*-(*N*-succinimidyl)uronium tetrafluoroborate (TSTU) (58 mg, 0.19 mmole). The reaction was stirred at room temperature. After 15 minutes, the reaction was analyzed by HPLC using a Phenomenex, C_{18} , 10 micron, 3.9×300 mm column and a 30 minute gradient of 10 → 70% MeCN–water (each with 0.05% TFA) at a flow rate of 1.0 mL per minute and UV detection at 260 nm. Clean conversion to the *N*-hydroxysuccinimide (NHS) ester of **6** eluting at 21.3 minutes was observed. The solution of the NHS ester was cooled to 4 °C and was added dropwise to an ice-cold solution of compound **7**³ (0.216 g, 0.48 mmole, HBr salt) dissolved in a mixture (5 mL) of 0.25 M sodium bicarbonate (85%) and DMF (15%). The reaction was warmed to room temperature and stirred for 30 minutes. HPLC analysis of the reaction mixture as described above showed clean conversion to product **8** eluting at 14 minutes. The product was purified by preparative HPLC as described for compound **2**. Yield = 82 mg (85%); red hygroscopic solid. $\nu_{\max}/\text{cm}^{-1}$ 3446 (NH), 1748 and 1662 (CO), 1473, 1202, 1176. δ_{H} (500 MHz, CF_3COOD) 1.52 (d, 6H, $J = 6.0$), 2.39 (br m, 2H), 2.55 (br s, 12H), 2.88 (br s, 2H), 3.23 (s, 3H), 3.31 (s, 6H), 3.43 (br m, 6H), 3.55–4.06 (m, 16H), 4.91 (spt, 1H, $J = 6.0$), 5.74 (m, 2H), 7.70 (br s, 2H), 7.86 (br s, 1H), 8.10 (m, 1H), 8.22 (m, 1H), 8.45 (m, 1H), 8.67 (m, 2H), 8.72 (d, 1H, $J = 9.0$); MALDI-TOF MS m/z 994.5 ($\text{M} + \text{H}$)⁺, HRMS m/z 993.4141 M^+ (993.4136 calculated).

Compound 9. A solution of compound **8** (62 mg, 0.062 mmole) in DMF (3 mL) and water (0.3 mL) was treated with diisopropylethylamine (0.054 mL, 0.31 mmole) and glutaric anhydride (36 mg, 0.31 mmole). The reaction was stirred at room temperature. After 30 minutes, the reaction was analyzed by HPLC using a Phenomenex, C_{18} , 10 micron, 3.9×300 mm column and a 30 minute gradient of 10 → 70% MeCN–water

(each with 0.05% TFA) at a flow rate of 1.0 mL per minute and UV detection at 260 nm. The glutarate derivative of compound **9** was observed eluting at 15.3 minutes (>80% conversion). The reaction mixture was then treated with diisopropylethylamine (0.13 mL, 0.75 mmole) and TSTU (0.26 g, 0.86 mmole). The reaction was stirred at room temperature. After 30 minutes, the reaction was analyzed by HPLC as described above. Product **9** was observed eluting at 16.5 minutes (>80% conversion). The product was purified by preparative HPLC as described for compound **2**. The HPLC fractions containing product **9** were frozen at $-80\text{ }^{\circ}\text{C}$ and lyophilized. Yield = 42 mg (56%); fluffy reddish-yellow solid. $\nu_{\text{max}}/\text{cm}^{-1}$ 1737, 1705, 1688 and 1680 (CO), 1202, 1136. δ_{H} (500 MHz, CF_3COOD) 1.55 (d, 6H, $J = 6.0$), 2.06–2.47 (m, 4H), 2.58 (br s, 10H), 2.67 (t, 2H, $J = 7.0$), 2.83 (t, 2H, $J = 7.0$), 2.86–2.96 (m, 2H), 3.08 (s, 4H), 3.22 (s, 3H), 3.33 (s, 6H), 3.45 (m, 4H), 3.59 (m, 6H), 3.71–3.90 (m, 10H), 3.94 (br t, 2H), 4.93 (spt, 1H, $J = 6.0$), 5.77 (m, 2H), 7.74 (s, 2H), 7.88 (s, 1H), 8.13 (br t, 1H), 8.25 (br d, 1H), 8.48 (br t, 1H), 8.69 (br d, 2H), 8.74 (d, 1H, $J = 9.0$). MALDI-TOF MS m/z 1204.8 M^+ ; HRMS m/z 1204.4670 M^+ (1204.4616 calculated).

Compound 12. A mixture of compound **10**¹⁴ (30 mg, 0.072 mmole), distilled 1,3-propane sultone (0.132 g, 1.08 mmole, 15 equivalents) and anhydrous sodium carbonate (38 mg, 0.36 mmole, 5 equivalents) in [BMIM][PF₆] (1 mL) was heated at $150\text{ }^{\circ}\text{C}$ under a nitrogen atmosphere. After 3 hours, an additional 15 equivalents of 1,3-propane sultone and 5 equivalents of sodium carbonate were added and the reaction was continued at $150\text{ }^{\circ}\text{C}$ for 3 hours. A final addition of 15 equivalents of 1,3-propane sultone and 5 equivalents of sodium carbonate was then performed and the reaction was continued at $150\text{ }^{\circ}\text{C}$ for 3 hours (total reaction time 9 hours). The reaction was then cooled to room temperature and analyzed by HPLC using a Phenomenex, C₁₈, 10 micron, 3.9×300 mm column and a 30 minute gradient of 10 \rightarrow 70% MeCN–water (each with 0.05% TFA) at a flow rate of 1.0 mL per minute and UV detection at 260 nm. Compound **11** was observed eluting as a broad peak at 14 minutes. The crude reaction mixture was partitioned between ethyl acetate (20 mL) and water (20 mL). The dark brown aqueous layer containing product was separated and washed once with ethyl acetate (20 mL). It was then concentrated under reduced pressure. Crude **11** was suspended in 1 M HCl (20 mL) and refluxed for 4 hours. It was then cooled to room temperature and analyzed by HPLC which showed complete conversion to product **12** eluting at 12.4 minutes. HPLC analysis of the reaction mixture using a Phenomenex C₈, 5 micron, 4.6×100 mm column and a 40 minute gradient of 10 \rightarrow 60% MeCN–water (each with 0.05% TFA) at a flow rate of 1 mL per minute showed product **12** eluting at 8.5 minutes. The product was purified by preparative HPLC as described for compound **2**. The HPLC fractions containing product were frozen at $-80\text{ }^{\circ}\text{C}$ and lyophilized. Yield = 30 mg (55%); dark yellow powder. $\nu_{\text{max}}/\text{cm}^{-1}$ 3477 (OH), 1751 and 1719 (CO), 1615, 1465, 1381, 1224, 1145. δ_{H} (500 MHz, CF_3COOD) 2.51 (s, 6H), 2.54 (br t, 4H), 2.84 (br s, 2H), 3.57 (t, 4H, $J = 7.0$), 3.74 (br t, 2H), 4.40 (t, 4H, $J = 5.0$), 5.76 (m, 2H), 7.78 (br s, 2H), 8.01 (s, 2H), 8.07 (d, 2H, $J = 10.0$),

8.75 (d, 2H, $J = 10.0$). MALDI-TOF MS m/z 769.4 M^+ ; HRMS m/z 770.1255 ($\text{M} + \text{H}$)⁺ (770.1247 calculated).

Compound 13. A solution of compound **12** (10 mg, 0.013 mmole) in DMF (1.5 mL) was treated with diisopropylethylamine (0.0068 mL, 0.04 mmole) and TSTU (6 mg, 0.02 mmole). The reaction was stirred at room temperature. After 30 minutes, the reaction was analyzed by HPLC using a Phenomenex, C₁₈, 10 micron, 3.9×300 mm column and a 30 minute gradient of 10 \rightarrow 70% MeCN–water (each with 0.05% TFA) at a flow rate of 1.0 mL per minute and UV detection at 260 nm. Product **13** was observed eluting at 14.5 minutes. The product was purified by preparative HPLC as described for compound **2**. The HPLC fractions containing product were frozen at $-80\text{ }^{\circ}\text{C}$ and lyophilized. Yield = 8.3 mg (93%); dark yellow solid. $\nu_{\text{max}}/\text{cm}^{-1}$ 3443 (OH), 1762, 1738 and 1615 (CO), 1464, 1382, 1317, 1200. δ_{H} (500 MHz, CF_3COOD) 2.58 (s, 6H), 2.60 (br s, 4H), 2.90 (br s, 2H), 3.19 (br s, 4H), 3.61 (t, 4H, $J = 7.0$), 3.80 (br t, 2H), 4.46 (br t, 4H), 5.82 (br t, 2H), 7.83 (br s, 2H), 8.08 (s, 2H), 8.14 (d, 2H, $J = 9.0$), 8.81 (d, 2H, $J = 9.0$). MALDI-TOF MS m/z 866.8 ($\text{M} + \text{H}$)⁺, HRMS m/z 867.1417 M^+ (867.1411 calculated).

2. Synthesis of anti-HBsAg antibody conjugates of **9**, **13** and **14** (Table 1)

A murine anti-HBsAg monoclonal antibody with a neutral pI was used for labeling with the acridinium ester labels **9**, **13** and **14**.

The monoclonal antibody (1 mg, 6.67 nanomoles, stock solution 6.2 mg mL^{-1} , 0.161 mL) was diluted with 0.24 mL of 0.1 M sodium carbonate, pH = 9. The protein solution was treated with DMSO solutions of acridinium esters as follows: for labeling with 5 and 10 equivalents of **14**, 0.0068 mL and 0.0136 mL of a 5 mg mL^{-1} DMSO solution were added; for labeling with 5 and 10 equivalents of **9**, 0.0081 and 0.0162 mL of a 5 mg mL^{-1} DMSO solution were added; and, for labeling with 5 and 10 equivalents of **13**, 0.0058 mL and 0.0116 mL of a 5 mg mL^{-1} DMSO solution were added. The labeling reactions were stirred at $4\text{ }^{\circ}\text{C}$ for ~ 3 hours and were then transferred to 4 mL Amicon™ filters (MW 30 000 cutoff) and diluted with 3.6 mL de-ionized water. The volume was reduced to ~ 0.25 mL by centrifuging at 4000g for 10 minutes. The concentrated conjugate solutions were diluted with 4 mL de-ionized water and centrifuged again to reduce the volume. This process was repeated a total of four times. Finally, the concentrated conjugates were diluted with ~ 0.25 mL de-ionized water and were frozen and lyophilized. The lyophilized conjugates were dissolved in 0.5 mL of de-ionized water. Label incorporation was measured by MALDI-TOF mass spectrometry using the Voyager-DE instrument from Perkin-Elmer. This entailed measuring the molecular weight of the unlabeled protein and the labeled protein. The acridinium ester label contributed to the observed difference in mass between these two measurements. By knowing the molecular weight of the specific acridinium ester label, the extent of label incorporation for that specific acridinium ester could thus be calculated. Label incorporation in each conjugate is tabulated in Table 1.

3. Emission wavelength measurements (Fig. 4)

Emission spectra of the acridinium esters **9**, **13** and **14** were measured using an FSSS (Fast Spectral Scanning System) camera (Spectra Scan Model 704) from Photo Research Inc. In a typical measurement, 0.05–0.1 mL of a 1 mg mL⁻¹ solution of the acridinium ester in a 2 : 1 mixture of water–MeCN (with 0.05% TFA) was diluted with 0.3 mL of reagent 1 comprising 0.5% hydrogen peroxide in 0.1 M nitric acid. Just prior to the addition of reagent 2 comprising 7 mM CTAC in 0.25 M sodium hydroxide, the shutter of the camera was opened and light was collected for 5 seconds. The output of the instrument is a graph of light intensity *versus* wavelength.

4. UV-Visible spectrophotometric measurements (Fig. 5)

UV-Visible spectrophotometry of acridinium esters **9**, **13** and **14** for determination of the pK_a of the acridinium to pseudo-base transition was carried out by dissolving the HPLC-purified acridinium esters in DMSO (~1 mg mL⁻¹). These solutions were further diluted 20-fold into 0.2 M phosphate or borate buffer at pH 2, 3.0, 4.0, 5.0, 6.0, 7.0, 8.0, 9.0 and 10.0 (8–10 only for compound **13**, pH 10 was 0.2 M borate buffer). A solution of 0.1 M HCl was used for pH 1. The diluted acridinium ester solutions were allowed to stand for one hour at room temperature (**9** and **14**) or 16 hours (**13**) and then UV-Visible spectra were recorded from 220–500 nm. The absorption intensity of the acridinium band at 383 nm for compounds **9**, **14** and 410 nm for compound **13** was measured as a function of pH. A plot of this data is shown in Fig. 5.

5. Chemiluminescence measurements (Fig. 6, 7, S10[†])

Chemiluminescence of acridinium esters **9**, **13** and **14** and their anti-HBsAg antibody conjugates was measured on an AutoLumat LB953 Plus luminometer from Berthold Technologies. HPLC-purified acridinium esters **9**, **13** and **14** were initially dissolved in DMSO (1–2 mg mL⁻¹), allowed to stand for several hours and were further diluted for chemiluminescence measurements in an aqueous buffer of 10 mM disodium hydrogen phosphate, 0.15 M NaCl, 8 mM sodium azide and 0.015 mM bovine serum albumin (BSA), pH = 8.0. Protein conjugates, ~2 mg mL⁻¹ were serially diluted 10⁵-fold for chemiluminescence measurements. Similarly, solutions of acridinium ester labels were serially diluted 10⁶-fold for chemiluminescence measurements. A 0.010 mL volume of each diluted acridinium ester or conjugate sample was dispensed into the bottom of a cuvette. Cuvettes were placed in the primed LB953 and the chemiluminescence reaction was initiated with the sequential addition of 0.3 mL of reagent 1, a solution of 0.5% hydrogen peroxide in 0.1 M nitric acid, followed by the addition of 0.3 mL of reagent 2, a solution of 0.25 M sodium hydroxide with or without CTAC surfactant. Each chemiluminescence flash curve was measured in 100 intervals of 0.1 second (10 seconds total time) in the presence of 7 mM CTAC or 240 intervals of 0.5 second (2 minutes total time) in the absence of CTAC from the point of chemiluminescence initiation with the addition of 0.25 M NaOH. Each

chemiluminescence reaction was carried out a minimum of three times, averaged and converted to a percentage of the chemiluminescence accumulated up to each time interval. The output from the luminometer instrument was expressed as RLUs (relative light units).

6. Isoelectric focusing (IEF) gel electrophoresis

Isoelectric focusing (IEF) gel electrophoresis of the anti-HBsAg antibody and the acridinium ester conjugates was performed using an XCell SureLock Mini-Cell (Life Technologies) and Novex 3-10 IEF gels (Life Technologies) and Novex buffers. IEF markers, pH 3–10 (Life Technologies), were used as reference standards. Conjugates (~2 mg mL⁻¹) were mixed 1 : 1 with Novex IEF sample buffers pH 3–10 and 0.012 mL was loaded onto the gel. The gel was run at 100 volts for 1 hour, 200 volts for 1 hour and then 500 volts for 30 minutes. The gel was then fixed for 30 minutes using 12% trichloroacetic acid and 3.5% sulfosalicylic acid. The gel was stained for 15 minutes in Coomassie Blue R-250 and then doubly stained overnight with 30% methanol, 10% acetic acid in de-ionized water.

7. Measurement of fractional non-specific binding (FNSB) (Table 2)

The fractional non-specific binding (FNSB) of anti-HBsAg antibody conjugates of acridinium ester labels **9**, **13** and **14** was measured using a Siemens Healthcare Diagnostics' ADVIA Centaur® automated immunoanalyzer. The conjugates were diluted to equivalent concentrations of 10 nM in a solution consisting of 0.1 M sodium *N*-(2-hydroxyethyl) piperazine-*N'*-2-ethanesulfonate (HEPES), 0.15 M sodium chloride, 7.7 mM sodium azide, 12 mM *t*-octylphenoxypolyethoxyethanol (Triton X-100), 0.076 mM BSA, pH = 7.7. A volume of 0.1 mL each of these 10 nM protein–acridinium ester conjugate solutions were mixed with 0.1 mL of horse serum and 0.2 mL of either of three solid phases. The first solid phase was 0.35 grams per liter paramagnetic microparticles (PMP) covalently covered with mouse anti-fluorescein antibody. The second solid phase was 0.35 grams per liter of Dynabeads® M-280 magnetic latex particles (Life Technologies) covalently covered with streptavidin. The third solid phase was 0.35 grams per liter of Dynabeads® M-270 magnetic latex particles (Life Technologies) covalently covered with streptavidin. After an incubation of 5.5 minutes to allow interaction between the acridinium ester conjugate and the solid phases, the solid phases were magnetically collected and washed twice with either water or a buffer of 10 mM potassium phosphate, 0.14 M sodium chloride, 14 mM sodium azide, 1 mM EDTA (ethylenediaminetetraacetic acid), 0.8 mM Tween 20 (polyoxyethylene-20 sorbitan monolaurate), pH = 7.2. The chemiluminescence, expressed as RLUs, of both the input acridinium ester chemiluminescence and the chemiluminescence of the acridinium ester associated with the particles was measured for 4 seconds on the ADVIA Centaur® with sequential addition of 0.3 mL each of reagent 1 (0.1 M nitric acid and 0.5% hydrogen peroxide) and reagent 2 (0.25 M sodium hydroxide containing 7 mM cetyltrimethylammonium chloride). FNSB was calculated as the ratio of

particle-bound chemiluminescence to input chemiluminescence by averaging the chemiluminescence of ten measurements.

8. Measurement of chemiluminescence stability (Fig. 9)

Acridinium ester anti-HBsAg antibody conjugates of labels **9**, **13** and **14** were diluted to a concentration of 0.1 nM in a buffer of 0.1 M sodium *N*-(2-hydroxyethyl) piperazine-*N'*-2-ethanesulfonate (HEPES), 0.15 M sodium chloride, 7.7 mM sodium azide, 12 mM *t*-octylphenoxypolyethoxyethanol (Triton X-100), 0.076 mM BSA at pH = 6.0 or pH 7.4. The diluted conjugates were kept at 4 and 37 °C for four weeks. The residual chemiluminescence of each diluted conjugate was assessed over the course of the four weeks by periodically averaging the 5 second chemiluminescence measurement of five 0.01 mL samples on the AutoLumat LB953 Plus luminometer with sequential addition of 0.3 mL each of reagent 1 (0.1 M nitric acid and 0.5% hydrogen peroxide) and reagent 2 (0.25 M sodium hydroxide containing 7 mM cetyltrimethylammonium chloride). The change in chemiluminescence was gauged against initial values as a percentage.

Acknowledgements

We thank Ms Elzbieta Rotter-Wask for the IEF gel of the antibody conjugates. We also thank Mr David Wen for IR spectra of synthetic compounds and for helpful suggestions with the manuscript.

References

- (a) S.-J. Law, C. S. Leventis, A. Natrajan, Q. Jiang, P. B. Connolly, J. P. Kilroy, C. R. McCudden and S. M. Tirrell, *US Pat.*, 5,656,426, 1997; (b) A. Natrajan, D. Sharpe and Q. Jiang, *US Pat.*, 6,664,043 B2, 2003; (c) A. Natrajan, D. Sharpe, J. Costello and Q. Jiang, *Anal. Biochem.*, 2010, **406**, 204–213; (d) A. Natrajan, D. Sharpe and D. Wen, *Org. Biomol. Chem.*, 2012, **10**, 1883–1895.
- (a) F. McCapra, *Acc. Chem. Res.*, 1976, **9/6**, 201–208; (b) F. McCapra, D. Watmore, F. Sumun, A. Patel, I. Beheshti, K. Ramakrishnan and J. Branson, *J. Biolumin. Chemilumin.*, 1989, **4**, 51–58; (c) J. Rak, P. Skurski and J. Błażejowski, *J. Org. Chem.*, 1999, **64**, 3002–3008; (d) K. Krzyński, A. Ożóg, P. Malecha, A. D. Roshal, A. Wróblewska, B. Zadykiewicz and J. Błażejowski, *J. Org. Chem.*, 2011, **76**, 1072–1085.
- A. Natrajan, D. Sharpe and D. Wen, *Org. Biomol. Chem.*, 2011, **9**, 5092–5103.
- A. Natrajan, D. Sharpe and D. Wen, *Org. Biomol. Chem.*, 2012, **10**, 3432–3447.
- (a) I. Weeks, I. Beheshti, F. McCapra, A. K. Campbell and J. S. Woodhead, *Clin. Chem.*, 1983, **29/8**, 1474–1479; (b) J. W. Bunting, V. S. F. Chew, S. B. Abhyankar and Y. Goda, *Can. J. Chem.*, 1984, **62**, 351–354; (c) P. W. Hammond, W. A. Wiese, A. A. Waldrop III, N. C. Nelson and L. J. Arnold Jr., *J. Biolumin. Chemilumin.*, 1991, **6**, 35–43.
- A. Natrajan, T. Sells, H. Schroeder, G. Yang, D. Sharpe, Q. Jiang, H. Lukinsky and S.-J. Law, *US Pat*, 7,319,041, 2008.
- (a) T. Kinkel, H. Lübbbers, E. Schmidt, P. Molz and H. J. Skrzypczyk, *J. Biolumin. Chemilumin.*, 1989, **4**, 136–139; (b) P. G. Mattingly, *J. Biolumin. Chemilumin.*, 1991, **6**, 107–114.
- S.-J. Law, T. Miller, U. Piran, C. Klukas, S. Chang and J. Unger, *J. Biolumin. Chemilumin.*, 1989, **4**, 88–98.
- A. Natrajan and D. Wen, *Green Chem.*, 2011, **13**, 913–921.
- R. C. Brown, Z. Li, A. J. Rutter, X. Mu, O. H. Weeks, K. Smith and I. Weeks, *Org. Biomol. Chem.*, 2009, **7**, 386–394.
- S. Caddick, J. D. Wilden and D. B. Judd, *J. Am. Chem. Soc.*, 2004, **126**, 1024–1025.
- J. D. Wilden, D. B. Judd and S. Caddick, *Tetrahedron Lett.*, 2005, **46**, 7637–7640.
- (a) A. T. Ślósarczyk and L. Baltzer, *J. Pept. Sci.*, 2012, **18**, 261–269; (b) A. T. Ślósarczyk, R. Ramapanicker, T. Norberg and L. Baltzer, *RSC Adv.*, 2012, **2**, 908–914.
- A. Natrajan, Q. Jiang, D. Sharpe and J. Costello, *US Pat.*, 7,309,615 B2, 2007.
- K. A. Browne, D. D. Deheyn, G. A. El-Hiti, K. Smith and I. Weeks, *J. Am. Chem. Soc.*, 2011, **133**, 14637–14648.
- (a) F. McCapra, *J. Chem. Soc., Chem. Commun.*, 1977, 946–948; (b) F. McCapra, I. Beheshti, A. Burford, R. A. Hann and K. A. Zaklika, *J. Chem. Soc., Chem. Commun.*, 1977, 944–946.
- G. B. Schuster, *Acc. Chem. Res.*, 1979, **12**, 366–373.
- D. E. Garfin, in *Gel Electrophoresis of Proteins, Essential Cell Biology, Volume 1, Cell Structure: A Practical Approach*, ed. J. Davey and M. Lord, Oxford University Press, 2003, pp. 197–268.
- (a) R. C. Chapman, E. Ostuni, L. Yan and G. M. Whitesides, *Langmuir*, 2000, **16**, 6927–6936; (b) R. C. Chapman, E. Ostuni, M. N. Liang, G. Meluleni, E. Kim, L. Yan, G. Pier, H. S. Warren and G. M. Whitesides, *Langmuir*, 2001, **17**, 1225–1233; (c) S. J. Sofia, V. Premnath and E. W. Merrill, *Macromolecules*, 1998, **31**, 5059–5070; (d) Y.-H. Zhao, B.-K. Zhu, L. Kong and Y.-Y. Xu, *Langmuir*, 2007, **23**, 5779–5786; (e) A. R. Denes, E. B. Somers, A. C. L. Wong and F. Denes, *J. Appl. Polym. Sci.*, 2001, **81**, 3425–3438; (f) J. Ladd, Z. Zhang, S. Chen, J. C. Hower and S. Jiang, *Biomacromolecules*, 2008, **9**, 1357–1361; (g) Y. Chang, S. Chen, Z. Zhang and S. Jiang, *Langmuir*, 2006, **22**, 2222–2226; (h) Z. Zhang, T. Chao, S. Chen and S. Jiang, *Langmuir*, 2006, **22**, 10072–10077; (i) W. K. Cho, B. Kong and I. S. Choi, *Langmuir*, 2007, **23**, 5678–5682; (j) G. Cheng, Z. Zhang, S. Chen, J. D. Bryers and S. Jiang, *Biomaterials*, 2007, **28**, 4192–4199; (k) H. Kitano, A. Kawasaki, H. Kawasaki and S. Morokoshi, *J. Colloid Interface Sci.*, 2005, **282**, 340–348.